



Article

Deep Feature Extraction for *Cymbidium* Species Classification Using Global–Local CNN

Qiaojuan Fu, Xiaoying Zhang, Fukang Zhao, Ruoxin Ruan, Lihua Qian and Chunnan Li *

Hangzhou Academy of Agricultural Sciences, Hangzhou 311400, China; fqjwxj@126.com (Q.F.); zxiaoying2013@163.com (X.Z.); zfk@hz.cn (F.Z.); buffalo126@126.com (R.R.); menoy@hz.cn (L.Q.)

* Correspondence: goodjian123@gmail.com

Abstract: *Cymbidium* is the most famous and widely distributed type of plant in the *Orchidaceae* family. It has extremely high ornamental and economic value. With the continuous development of the *Cymbidium* industry in recent years, it has become increasingly difficult to classify, identify, develop, and utilize orchids. In this study, a classification model GL-CNN based on a convolutional neural network was proposed to solve the problem of *Cymbidium* classification. First, the image set was expanded by four methods (mirror rotation, salt-and-pepper noise, image sharpening, and random angle flip), and then a cascade fusion strategy was used to fit the multiscale features obtained from the two branches. Comparing the performance of GL-CNN with other four classic models (AlexNet, ResNet50, GoogleNet, and VGG16), the results showed that GL-CNN achieves the highest classification prediction accuracy with a value of 94.13%. This model can effectively detect different species of *Cymbidium* and provide a reference for the identification of *Cymbidium* germplasm resources.

Keywords: *Cymbidium*; classification; global–local CNN; convolutional neural network



Citation: Fu, Q.; Zhang, X.; Zhao, F.; Ruan, R.; Qian, L.; Li, C. Deep Feature Extraction for *Cymbidium* Species Classification Using Global–Local CNN. *Horticulturae* **2022**, *8*, 470. <https://doi.org/10.3390/horticulturae8060470>

Academic Editor: Jianwei Qin

Received: 12 April 2022

Accepted: 27 April 2022

Published: 25 May 2022

Publisher's Note: MDPI stays neutral with regard to jurisdictional claims in published maps and institutional affiliations.



Copyright: © 2022 by the authors. Licensee MDPI, Basel, Switzerland. This article is an open access article distributed under the terms and conditions of the Creative Commons Attribution (CC BY) license (<https://creativecommons.org/licenses/by/4.0/>).

1. Introduction

Orchidaceae is one of the largest and most diverse flowering plants and has been widespread all around the world [1]. *Cymbidium*, belonging to the *Orchidaceae* family, with elegant and upright leaves and fragrant flowers, is the most important and economic flowering genus. It is popular in Asia, especially in China, Japan, Korea, and Southeast Asia [2]. In China, the *Cymbidium* has more than a thousand years of history with extremely high cultural and economic value [3]. The flowers of *Cymbidium* have various colors and shape patterns, which usually leads to confusion when comparing cultivars to assess genetic resources at the species level [4]. In recent years, with the continuous development of the *Cymbidium* industry, the number of *Cymbidium* germplasm resources has increased year by year, which greatly increases the difficulty of orchid classification, identification, and development. Traditional approaches for the classification of *Cymbidium* cultivars are based on morphological traits, which are difficult due to the problems associated with morphological variability, growth conditions, overlapping geographical origins, and individual biases, and most of these cultivars are related [5–7]. It requires professionals but offers jugged with subjective. Molecular recognition is the most effective method to identify the various *Cymbidium* cultivars [8–10], but often time and cost-consuming, making it unsuitable for high throughput and rapid classification.

Recently, an emerging field of machine learning, deep learning (DL), known as deep neural networks, has been growing fast and widely used in many fields, such as image processing, content prediction, and text understanding [11]. The main core of the deep learning algorithm is largely inherited from artificial neural network architecture with many hidden layers. Deep learning allows computers to process and analyze images and extract image details similar to the human brain and has been significantly progressed for image pattern recognition as computer vision algorithms [12]. Convolutional neural network (CNN) is one of the most common methods for visual image classification and has been

widely adopted by the research community [13]. With the support of powerful graphics processing units (GPU), CNN can be easily used with low-cost normal image data and huge numbers of datasets, as deep learning often requires large datasets and powerful resources for model training [14]. Inspired by the results of image classification and object detection, many researchers use CNN to identify plant images [15,16]. For instance, CNN has been successfully used to automatically learn discriminative features from leaf images [17] and to detect the diversity in flower images [18]. In addition, the features extracted by CNN could highly improve classification accuracy and have been suggested to be the optimal candidate for any visual task [19,20]. CNN has been successfully used to extract features for hyperspectral image (HSI) classification and perform at high accuracy [21]. Hiary et al. [22] conducted a two-step deep learning model that could automatically discover the portions of flowers and use the feature extracted from this portion to yield a high classification accuracy of 97.1% on flowers. Dias et al. [23] also performed feature extraction from a fine-tuned CNN model and used these features to establish a support vector machines (SVM) classification model. The model accuracy reached 90% on apple flowers. In addition, a combination of features extracted from pretrained CNN models (AlexNet, ResNet50, and VGG-16) was also used for flower species classification, with a success rate of 80%. These pretrained models have achieved successful results in an ImageNet competition [24]. Evidence has shown that combining the feature selection of CNN model and traditional machine learning methods, such as SVM and random forest (RF), could yield a high success rate, save massive process time, and reduce computation intensity [25]. However, among the available research into CNN technologies, there is limited research into detecting flower images of diverse *Cymbidium* species.

CNN has a powerful ability to capture local features and keep parallel motion unchanged [26]. However, the existing classification methods based on CNN mostly focus on single-scale image datasets [27]. Global–local CNN (GL-CNN), a CNN based on multifeature fusion, can fuse global and local features. Hao et al. [27] used GL-CNN to classify the growth period of *Gynura bicolor* DC, and the test accuracy of GL-CNN reached 95.63%. In this study, we proposed a global–local joint training CNN framework called GL-CNN to solve the problem of identifying different *Cymbidium* species instead of using global image information alone. Specific objectives were to: (1) The image set was expanded by four methods (mirror rotation, salt-and-pepper noise, image sharpening, and random angle flipping) to improve the model training effect and prevent overfitting. (2) A GL-CNN architecture based on a fusion strategy was proposed to classify 10 different species of *Cymbidium*. (3) The GL-CNN model was compared with the four classic models (AlexNet, ResNet50, GoogleNet, and VGG16) and the model performance was comprehensively evaluated.

2. Materials and Methods

2.1. *Cymbidium* Species Flower Dataset

In this study, we collected 10 species of *Cymbidium*, which were *C. goeringii*, *C. longibracteatum*, *C. faberi*, *C. sinense*, *C. hybrids*, *C. hybridum*, *C. ensifolium*, *C. kanran*, *C. hookerianum*, and *C. tortisepalum* for flower classification. During the flowering period, the flowers of each species were pictured using a high-definition camera (Canon 500D, Tokyo, Japan). There was a total of 3390 pictures. They were divided into two types, as shown in Figure 1. One was an unpicked *Cymbidium* plant, and the other was a flower on a black background.

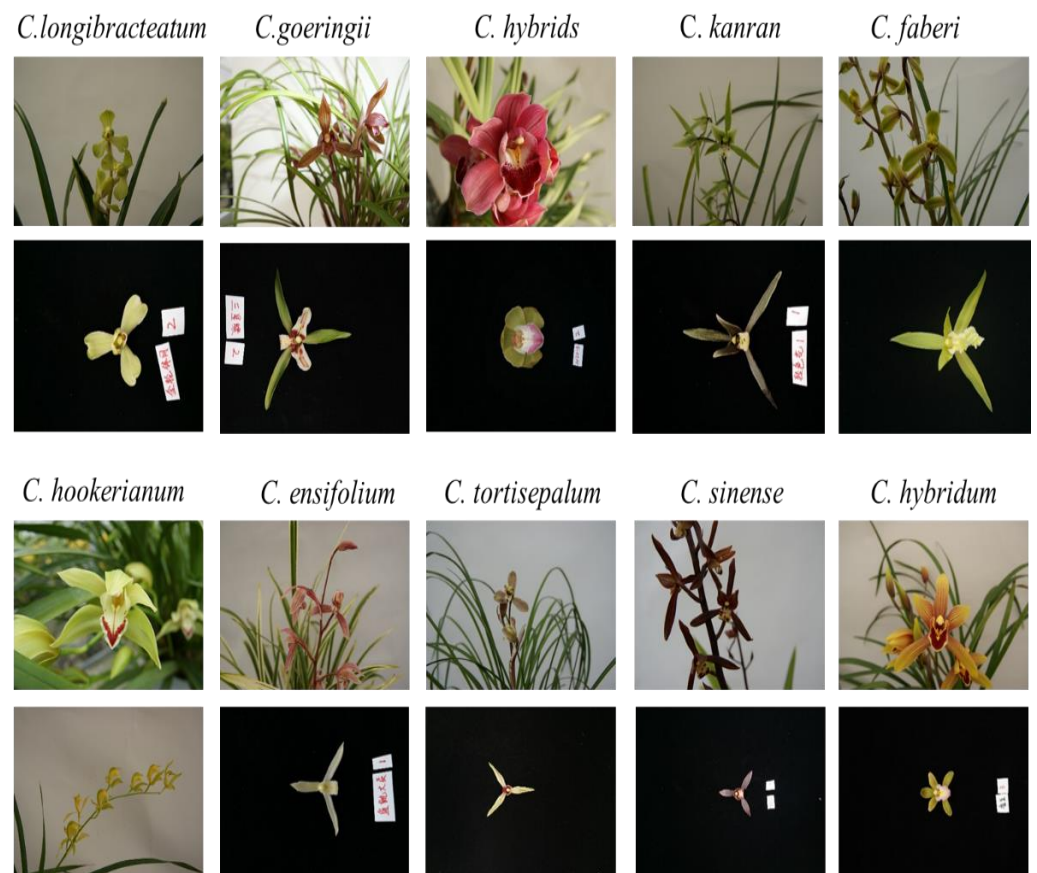


Figure 1. Examples of pictures of 10 *Cymbidium* species.

2.2. Data Preprocessing

2.2.1. Two-Scale Image Acquisition

Before model training, *Cymbidium* images were subjected to two-scale processing to improve the robustness of the classification model established by the image with different backgrounds [27]. Figure 2 shows an image sample randomly selected from 10 *Cymbidium* species. The red frame represents the second scale image captured. First, set the original image to a size of 224×224 to obtain an image of the first scale. Since the recognition targets were basically located in the middle of the images, the experiment chose to intercept a partial image from the center of the first scale image (the height and width of the partial image were both 0.8 times of the first scale image) as the second scale image. The size of the second scale image was the same as the first scale image, which was 224×224 [28].

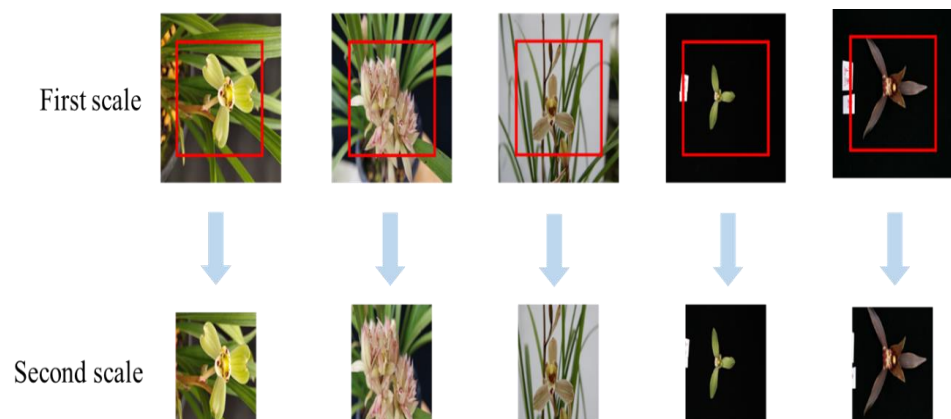


Figure 2. Schematic diagram of two-scale image acquisition.

2.2.2. Data Set Enhancement

The original data set was divided into training, validation, and test sets at a ratio of 8:1:1. Although the diversity of sample species and morphology were considered in the image collection process, the growth of orchids and the imaging angle were random [26]. This experiment mainly chose mirror rotation, sharpening, salt-and-pepper noise, and random angle rotation to enhance the image set [29–31]. The total number of samples was expanded by four times, and the effects before and after image enhancement are shown in Figure 3.



Figure 3. Examples of the effects before and after image enhancement.

2.3. Global–Local CNN Classification Model

2.3.1. GL-CNN Model Construction

In this part, we proposed a global–local CNN (GL-CNN) network to achieve accurate classification of different kinds of *Cymbidium*. The network consists of two types of features extracted from the trained GL-CNN. The first branch network is the global feature, denoted as “Gnet.” The second feature is used to capture the local information of the input image, denoted as “LNet” [27]. The overall network structure is shown in Figure 4. The model input consists of two parts. The original image is input to GNet with a size of 224×224 , and the corresponding local images of the same size are input to LNet. There is a one-to-one correspondence between input images of two scales. This operation expands the original image information from the data level by expanding the resolution of the input image in the LNet branch.

This experiment designed different sizes of convolution kernels according to the scale of the input image in order to enhance the feature extraction ability of the network. As shown in Figure 4, since GNet extracts global features based on larger-scale images, the size of the first convolution kernel is set to 11×11 to extract edge features. This branch mainly includes four convolutional layers, three pooling layers, and one fully connected layer. Moreover, LNet is a detailed feature extraction branch based on a more fine-grained

image design, which adds an additional convolutional layer based on GNet to abstract the features [26].

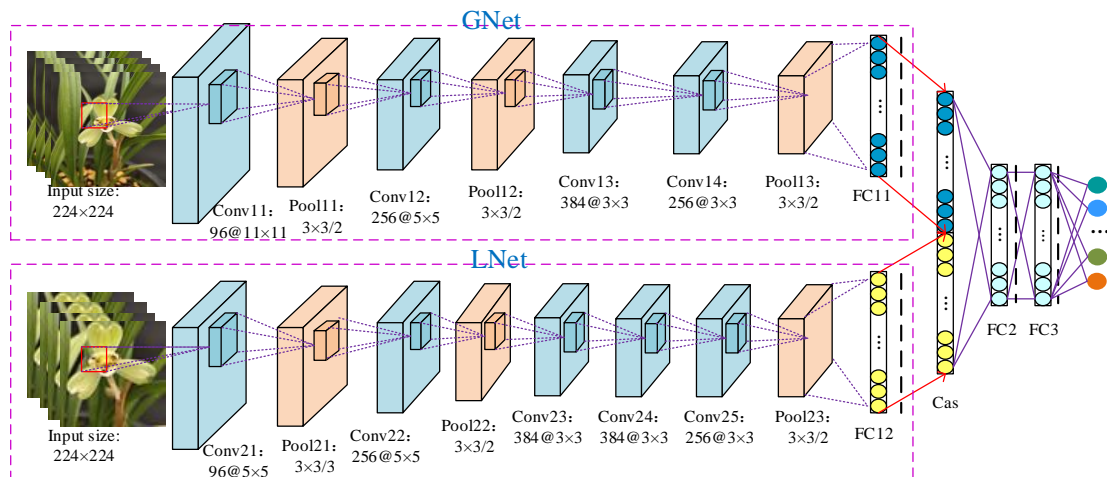


Figure 4. GL-CNN network structure diagram.

2.3.2. Cascade Fusion Strategy

We used the cascade fusion strategy to fit the multiscale features obtained from the two branches [32]. A feature fusion block was designed to capture features with more details [31]. With a cascading operation, it can process data layer-by-layer, and it only merges the two parts of the feature vectors without performing other mathematical operations. More importantly, the concatenated vector contains all the feature vectors. In a nutshell, the model can be concerned as an “ensemble of ensembles.”

In order to combine the different features of the global image and the local image, the “cascade fusion” strategy integrates FC11 and FC12 into the Cas layer through cascade (Table 1) and sends the Cas feature queue to the FC2 and FC3 layers for further feature combination and integration. Finally, the prediction probability output is realized through the SoftMax layer. The main hidden layer parameter settings are shown in Table 1.

Table 1. Details of GL-CNN hidden layer parameters.

Layer	Type	Size	Number of Cores	Step Size	Output Size	Number of Convolutions	Number of Neurons
Input	-	-	-	-	224 × 224 × 3	-	-
Conv11	Convolution	11 × 11	96	4	54 × 54 × 96	(11 × 11 + 1) × 96	54 × 54 × 96
Pool11	Mean-pooling	3 × 3	-	2	26 × 26 × 96	-	26 × 26 × 96
Conv12	Convolution	5 × 5	96	1	26 × 26 × 256	(5 × 5 + 1) × 96	26 × 26 × 96
Pool12	Mean-pooling	3 × 3	-	2	12 × 12 × 96	-	12 × 12 × 96
Conv13	Convolution	3 × 3	192	1	12 × 12 × 384	(3 × 3 + 1) × 192	12 × 12 × 192
Conv14	Convolution	3 × 3	256	1	12 × 12 × 384	(3 × 3 + 1) × 256	12 × 12 × 256
Pool13	Mean-pooling	3 × 3	-	2	5 × 5 × 256	-	5 × 5 × 256
FC11	Fully connected	1 × 1	4096	-	1 × 1 × 4096	(1 × 1 + 1) × 4096	1 × 1 × 2048
Conv21	Convolution	5 × 5	96	3	75 × 75 × 96	(5 × 5 + 1) × 96	75 × 75 × 96
Pool21	Mean-pooling	3 × 3	-	3	25 × 25 × 96	-	25 × 25 × 96
Conv22	Convolution	5 × 5	96	1	25 × 25 × 256	(5 × 5 + 1) × 96	25 × 25 × 96
Pool22	Mean-pooling	3 × 3	-	2	12 × 12 × 96	-	12 × 12 × 96
Conv23	Convolution	3 × 3	192	1	12 × 12 × 384	(3 × 3 + 1) × 192	12 × 12 × 192
Conv24	Convolution	3 × 3	256	1	12 × 12 × 384	(3 × 3 + 1) × 256	12 × 12 × 256
Conv25	Convolution	3 × 3	256	1	12 × 12 × 384	(3 × 3 + 1) × 256	12 × 12 × 256
Pool23	Mean-pooling	3 × 3	-	2	5 × 5 × 256	-	5 × 5 × 256
FC21	Fully connected	1 × 1	4096	-	1 × 1 × 4096	(1 × 1 + 1) × 4096	1 × 1 × 2048
Cas	Cascade	-	-	-	1 × 1 × 8192	-	1 × 1 × 8192
FC2	Fully connected	1 × 1	4096	-	1 × 1 × 4096	(1 × 1 + 1) × 4096	1 × 1 × 4096
FC3	Fully connected	1 × 1	1000	-	1 × 1 × 1000	(1 × 1 + 1) × 1000	1 × 1 × 1000
Output	Output	1 × 1	10	-	1 × 1 × 10	-	-

2.3.3. Model Enhancement

The model uses ReLU6 and dropout to prevent gradient explosion and alleviate potential overfitting problems. End-to-end training is achieved through momentum stochastic gradient descent, and cross-entropy is used as the loss function.

ReLU 6 is an activation function commonly used in deep convolutional neural networks [27,33]. ReLU uses x for linear activation in the region of $x > 0$, which may cause the value after activation to be too large and affect the stability of the model [34]. In order to offset the linear growth of the ReLU excitation function, the ReLU6 function can be used. The ReLU activation function and derivative function are:

$$\text{ReLU6}(x) = \min(\max(x, 0), 6) \in [0, 6] \quad (1)$$

$$\text{ReLU6}'(x) = \begin{cases} 1, & 0 < x < 6 \\ 0, & \text{else} \end{cases} \in \{0, 1\} \quad (2)$$

Dropout is used to combat overfitting in artificial neural networks. It can avoid complicated mutual adaptation to training data [35]. During the network training process, half of the neurons are usually ignored randomly; that is, the dropout is set to 0.5. The cross-entropy loss function is used to evaluate the difference between the predicted and actual values of the model [36], which can be expressed as follows:

$$L = \frac{1}{N} \sum_i L_i = -\frac{1}{N} \sum_i \sum_{c=1}^M y_{ic} \log(p_{ic}) \quad (3)$$

where M is the number of categories, N is the number of samples, and y_{ic} indicates the symbolic function (0 or 1). If the true category of the sample i is equal to C , take 1, or otherwise take 0. p_{ic} indicates the predicted probability of the observation sample with i belonging to category C .

2.4. Model Training

2.4.1. Parameter Settings

Referring to the method of Hao et al. [27], the experiment was performed on a Windows 10 64-bit PC equipped with an Intel(R) Xeon(R) CPU @ 3.80 GHz processor, 32 GB RAM, and a GPU of NVIDIA GeForce GTX 3060. The GL-CNN model mentioned in this article is implemented based on the Keras framework. In addition, the maximum number of iterations epochs is set to 60, the initial learning rate is set to 0.05, and the learning rate is updated to 1/2 of the original value every 20 epochs. The "SGD+Momentum" strategy is adopted to update the parameters to improve the training speed of the model and avoid falling into the local optimum at the same time [37].

2.4.2. Contrast Experiment

In order to evaluate the performance of the proposed GL-CNN model in orchid-type classification tasks, comparative experiments were carried out with the classic AlexNet, ResNet50, GoogleNet, and VGG16 models. AlexNet is a convolutional neural network designed by Alex Krizhevsky and contains an eight-layer network [38]. The first five layers are convolutional layers, some of the later layers are maximum pooling layers, and the last three layers are fully connected layers. It uses a non-saturated ReLU activation function and shows better training performance than tanh and sigmoid [39]. The Residual Neural Network (ResNet) is an artificial neural network (ANN) that stacks residual blocks on top of each other to form a network. ResNet-50 is a convolutional neural network with a depth of 50 layers, which can accurately analyze visual images [40]. GoogLeNet is a type of convolutional neural network based on the Inception architecture [39]. It utilizes Inception modules, which allow the network to choose between multiple convolutional filter sizes in each block. An Inception network stacks these modules on top of each other, with occasional max-pooling layers with stride 2 to halve the resolution of the grid. VGG16 is a

convolutional neural network model proposed by K. Simonyan and A. Zisserman of Oxford University. This model achieves a top-five test accuracy rate of 92.7% in ImageNet [28].

2.4.3. Model Performance Evaluation

Four metrics, namely, precision, recall, F1-score, and accuracy, were used to evaluate the classification model [27,41], and the formulas are expressed as follows:

$$\text{Precision} = \frac{TP}{TP + FP} \quad (4)$$

$$\text{Recall} = \frac{TP}{TP + FN} \quad (5)$$

$$\text{Accuracy} = \frac{TP + TN}{TP + TN + FP + FN} \quad (6)$$

$$F1 = \frac{2TP}{2TP + FP + FN} \quad (7)$$

where true positive (TP) refers to the number of samples whose predicted value and actual value are both positive. False positive (FP) refers to the number of samples whose predicted value is positive, and the actual value is negative. False negative (FN) means false negative, which refers to the number of samples whose predicted value is negative, and the measured value is positive, correspondingly. True negative (TN) is true negative, which refers to the number of samples whose predicted value and actual value are both negative.

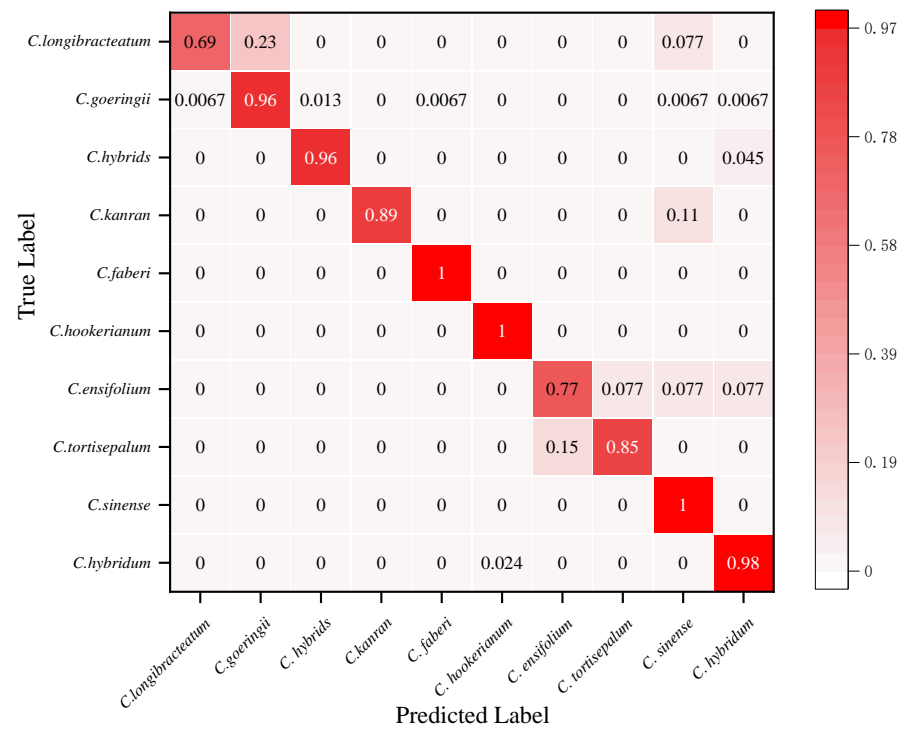
3. Results

3.1. Data Collection and Preprocessing

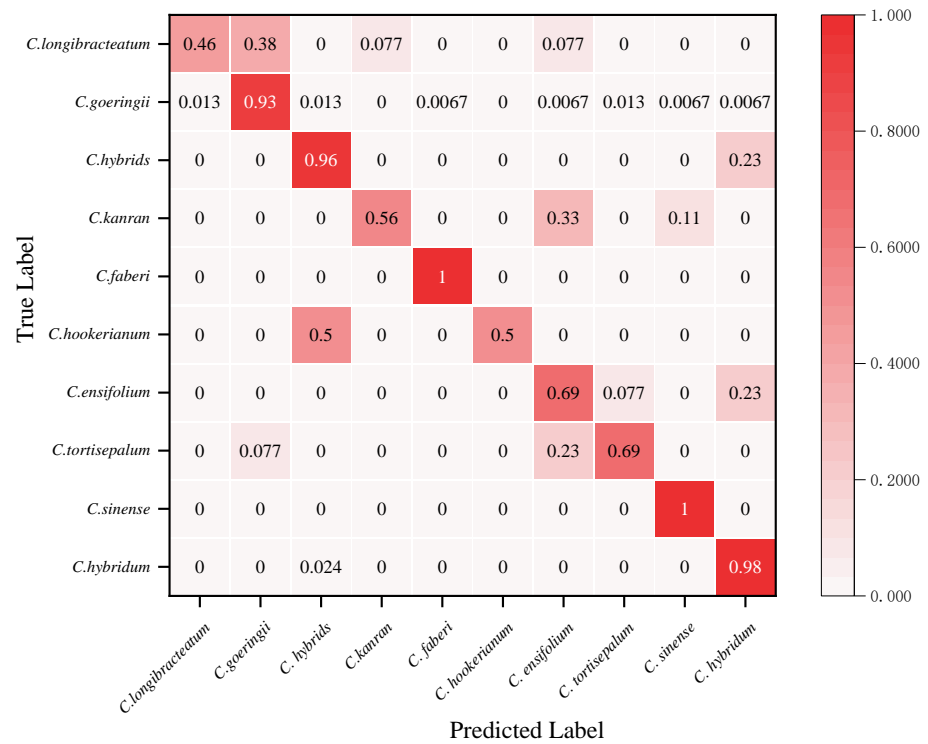
In the image samples randomly selected from 10 *Cymbidium* species shown in Figure 2, it can be observed that the background of the second scale image was smaller, and the details of the flower such as veins and textures were more abundant, which was more helpful to expand the input features and improve the classification accuracy. Four data enhancement methods, i.e., mirror rotation, sharpening, salt-and-pepper noise, and random angle rotation, were used to expand the training set by four times to prevent overfitting.

3.2. Model Performance Evaluation

The visual confusion matrix was used to count the classification results of different *Cymbidium* species (Figure 5). The true category (ordinates) and the predicted category (abscissa) were compared to obtain the classification rate of each species. The GL-CNN model has the highest prediction accuracy for *C. faberi* and *C. hookerianum*, with an accuracy rate of 100%, followed by *C. hybridum*, with an accuracy rate of 98% (Figure 5a). From the numerical distribution of the confusion matrix, it can be observed that all models have achieved high classification accuracy on *C. hybrids*, and their average classification rates have reached 95.6%. In addition, there have been more misclassifications between *C. goeringii*, *C. longibracteatum*, and *C. tortisepalum*. In general, the model GL-CNN built by this project has achieved a high individual classification rate in most orchid species recognition. The recognition performance of VGG16 is poor, and there is a serious misclassification phenomenon.

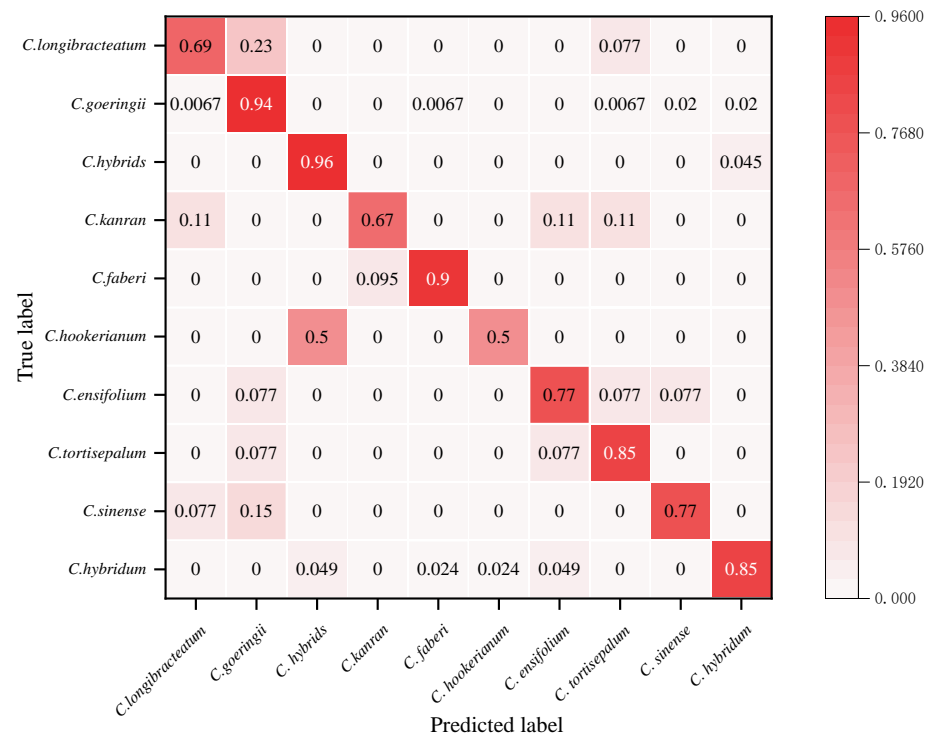


(a)

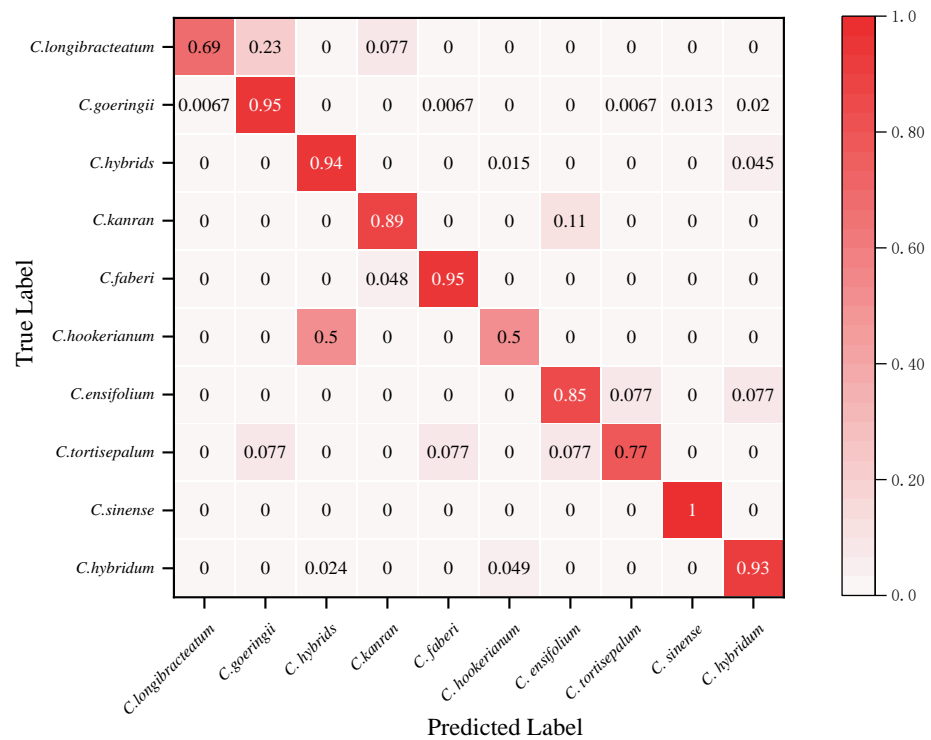


(b)

Figure 5. Cont.



(c)



(d)

Figure 5. Cont.

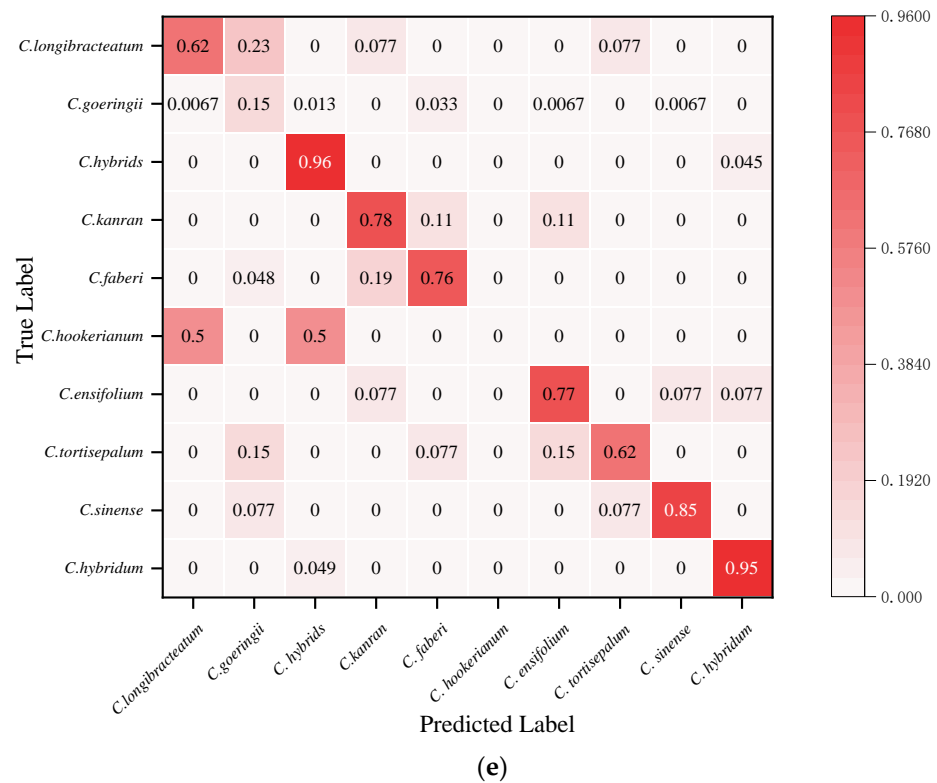


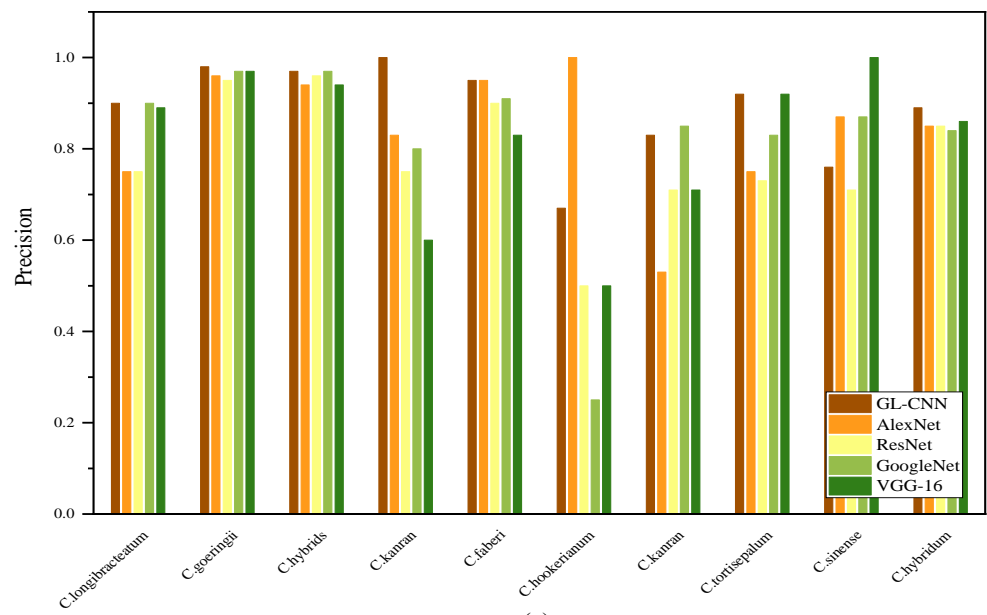
Figure 5. Test set confusion matrix: (a) GL-CNN; (b) AlexNet; (c) ResNet; (d) GoogleNet; (e) VGGNet.

Figure 6 shows the precision, recall, and F1-score of 5 models for classifying 10 *Cymbidium* species. Among them, the precision, recall, and F1-score of each model on *C. goeringii* and *C. hybrids* all reached high values. On the contrary, the precision, recall, and F1-score of the five models on the *C. hookerianum* are quite different. GL-CNN has the highest precision, with an average of 89%. ResNet’s average precision is the lowest, only 78%, indicating that there are many samples misclassified under this method. Using the AlexNet model, many samples were misclassified to other varieties (the average recall rate was 0.78) because the differences between the samples were small, and there was a certain degree of difficulty in recognition. The precision and recall rate of different models are quite different, which indicates that the recognition difference of each model is more prominent in the categories that are more difficult to distinguish, showing a certain degree of unstable performance. In addition, GL-CNN showed high precision and recall rates in 10 different species of *Cymbidium*, indicating its strong ability to extract nuances.

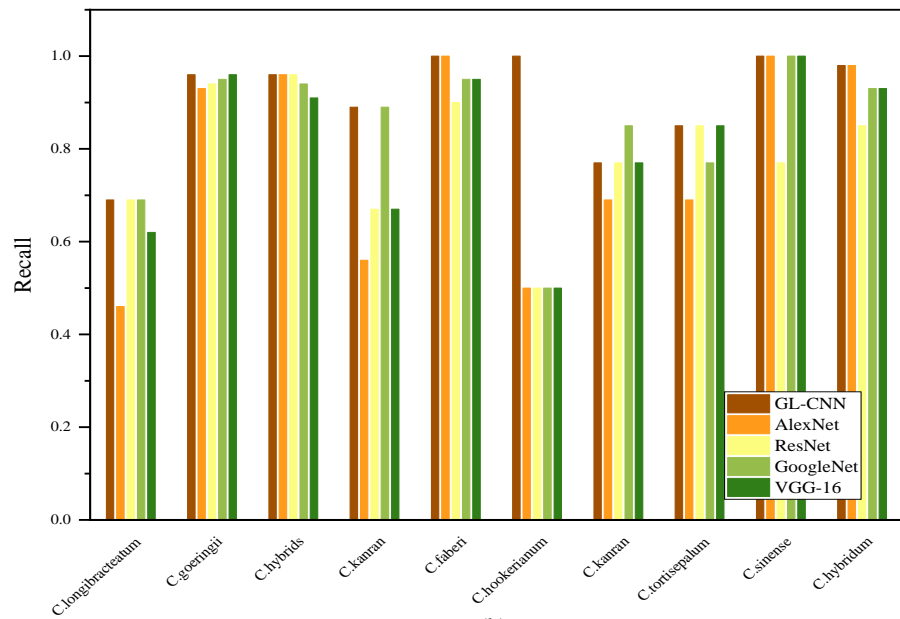
Table 2 lists the average accuracy of the five models in order to further and comprehensively evaluate the effectiveness of the model. It can be observed from the table that GL-CNN has achieved the highest average accuracy of 94.13%. Compared with other models, GL-CNN has greatly improved the accuracy of classification. Correspondingly, VGG16 only achieves an average accuracy of 88.60%, which is significantly lower than GL-CNN.

Table 2. Average accuracy of each model.

	GL-CNN	AlexNet	ResNet	GoogleNet	VGGNet
Average accuracy (%)	94.13	90.06	89.47	92.15	88.60



(a)



(b)

Figure 6. Cont.

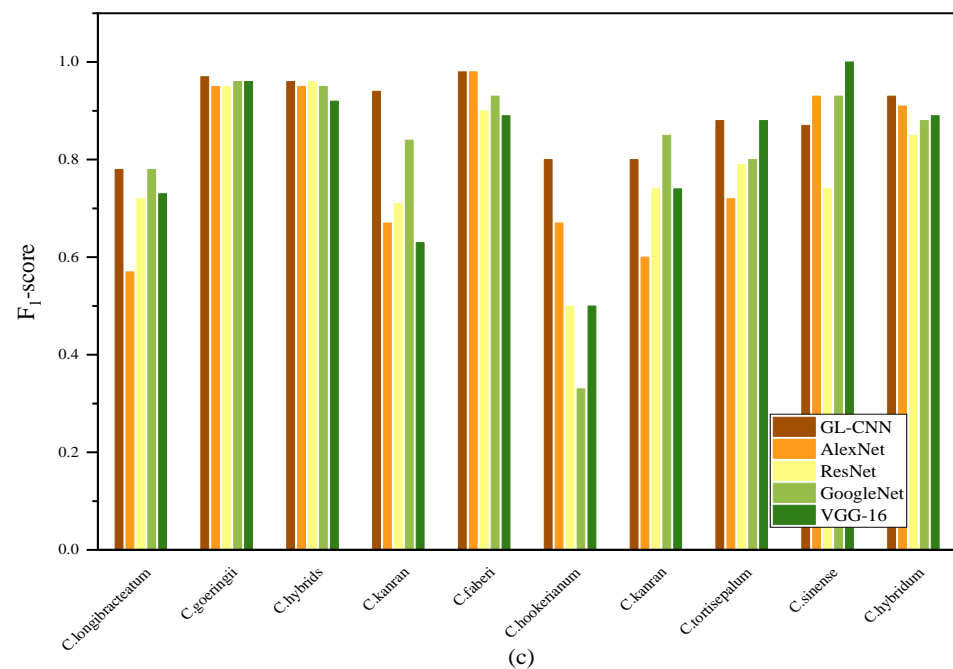


Figure 6. Precision (a), recall (b), and F1-score (c) of each model on different *Cymbidium* species.

4. Discussion

CNN is a method that combines an artificial neural network and deep learning with good fault tolerance and adaptability [42]. At the same time, it also has the advantages of automatic feature extraction, weight sharing, and a good combination of input image and network structure [27]. It is widely used in plant species identification, pest identification, weed identification, and other fields [43–45]. Existing CNN-based classification methods mainly focus on single-scale image data sets [27]. Therefore, there is an urgent need to design a fusion network that integrates the advantages of multiple features, which will greatly improve classification performance. This research proposed a two-scale CNN model, GL-CNN, which can extract features of different granularities from images of two scales, thereby enriching useful feature information, and ultimately improving the recognition ability of the model [26,27]. Researchers found that increasing the number of layers and units in the network will bring significant performance improvements, but it is prone to overfitting, explosion, or the disappearance of gradients [26]. To solve the above problems, a compact bilinear pooling method was proposed by Gao et al. [46], which can reduce the dimensionality while maintaining accuracy. Our experiment used a cascade fusion strategy to fit the two-scale features obtained from the two branches. Meanwhile, ReLU6, dropout, and other methods were used to alleviate potential overfitting problems. In the process of network training, dropout reduces the running time by randomly ignoring a certain proportion of hidden layer nodes, which can effectively reduce the interdependence between neurons, thereby extracting independent important features and inhibiting network overfitting.

In model training, the choice of feature extractor can affect the accuracy and speed of model detection. As the number of feature extractor layers increases, the network can extract higher-dimensional sample features, but the increase in network depth will affect the update signal of each layer and affect detection accuracy [47,48]. As classic feature extractors, AlexNet, ResNet, GoogleNet, and VGGNet are mostly used for image classification and recognition [48,49]. This study has shown that compared with the four typical models, GL-CNN has obvious accuracy and computational advantages, and the model accuracy is as high as 94%. An unexpected phenomenon is that the two excellent models (VGGNet and ResNet) did not achieve the desired performance, especially VGGNet, which obtained the lowest results, with a model accuracy of only 88.6%. The reason for

this phenomenon is that the VGGNet training speed is very slow, and the weight of the network architecture itself is very large. In the case of many parameters and insufficient image data, the excellent classification effect cannot be exerted [49,50]. ResNet's network connection is also very complicated and requires a lot of calculations. Therefore, they need a large data set to complete the convergence of the model [50]. In contrast, GoogLeNet, and AlexNet contain fewer parameters, a relatively simpler structure, and better training effects than VGGNet and ResNet [27]. As the best training model, GL-CNN has a slight advantage over GoogleNet in accuracy. The parameters and calculations of GL-CNN are significantly smaller, and it is easy to construct and apply. When the orchid image with more background information is adjusted to 224×224 , a great deal of fine-grained information will be lost, which prevents the network from learning more in-depth and sufficient details. This situation can lead to poor network performance. GL-CNN can obtain global and local information and cascade the two parts together to extract detailed context features, which helps to expand the input features and improve classification accuracy.

Deep learning is still data-driven, and the size and quality of the data set will directly affect the effectiveness of network training [26]. Due to the limitation of the data set size, it may be difficult to train CNN. This study found that the precision, recall, and F1-score of each model on *C. hookerianum* are quite different. This is due to the small sample size of *C. hookerianum*, which makes the stability performance of the model different. Therefore, the training model is not sensitive enough to recognize the experimental samples. By increasing the number of such images, the compatibility of the classification model for different *Cymbidium* species can be improved.

5. Conclusions

In this study, a *Cymbidium* classification method based on the GL-CNN was proposed. It consists of two CNN networks with comparable weight, which helps expand the input features and improve classification accuracy. The cascade fusion strategy was used to fit the multiscale features obtained from the two branches. ReLU6 and dropout were used to prevent gradient explosion and alleviate the problem of overfitting. The end-to-end training was realized, and the robustness of the model was enhanced. Comparing GL-CNN with four classic models (AlexNet, ResNet50, GoogleNet, and VGG16), the results showed that GL-CNN achieved the highest classification prediction accuracy with a value of 94.13%.

In summary, the GL-CNN model used in this paper integrates multiscale information through the network, expands the number of features, has high detection accuracy, and can effectively identify different species of *Cymbidium*.

Author Contributions: Q.F. and C.L. conceived the ideas and designed the methodology; Q.F. collected and analyzed the data and wrote the manuscript; C.L. guided the data analysis and reviewed the manuscripts; F.Z., R.R., L.Q., X.Z. and C.L. supervised all stages of the experiment. All authors have read and agreed to the published version of the manuscript.

Funding: This research was supported by the Hangzhou Agriculture and Social Development Project (20201203B104).

Institutional Review Board Statement: Not applicable.

Informed Consent Statement: Not applicable.

Data Availability Statement: Data are contained within the article.

Conflicts of Interest: The authors declare no conflict of interest.

References

1. Dressler, R.L. *Phylogeny and Classification of the Orchid Family*; Cambridge University Press: Cambridge, UK, 1993.
2. Sharma, S.K.; Rajkumari, K.; Kumaria, S.; Tandon, P.; Rao, S.R. Karyo-morphological characterization of natural genetic variation in some threatened *Cymbidium* species of Northeast India. *Caryologia* **2010**, *63*, 99–105. [[CrossRef](#)]
3. Lee, Y.-M.; Kim, M.-S.; Lee, S.-I.; Kim, J.-B. Review on breeding, tissue culture and genetic transformation systems in *Cymbidium*. *J. Plant Biotechnol.* **2010**, *37*, 357–369. [[CrossRef](#)]
4. Wang, H.-Z.; Lu, J.-J.; Hu, X.; Liu, J.-J. Genetic variation and cultivar identification in *Cymbidium ensifolium*. *Plant Syst. Evol.* **2011**, *293*, 101–110. [[CrossRef](#)]
5. Ning, H.; Ao, S.; Fan, Y.; Fu, J.; Xu, C. Correlation analysis between the karyotypes and phenotypic traits of Chinese *Cymbidium* cultivars. *Hortic. Environ. Biotechnol.* **2018**, *59*, 93–103. [[CrossRef](#)]
6. Guo, F.; Niu, L.-X.; Zhang, Y.-L. Phenotypic Variation of Natural Populations of *Cymbidium faberi* in Zhashui. *North Hortic.* **2010**, *18*, 91–93.
7. Sharma, S.K.; Kumaria, S.; Tandon, P.; Rao, S.R. Assessment of genetic variation and identification of species-specific ISSR markers in five species of *Cymbidium* (Orchidaceae). *J. Plant Biochem. Biotechnol.* **2013**, *22*, 250–255. [[CrossRef](#)]
8. Lu, J.; Hu, X.; Liu, J.; Wang, H. Genetic diversity and population structure of 151 *Cymbidium sinense* cultivars. *J. Hortic. For.* **2011**, *3*, 104–114.
9. Lee, D.-G.; Koh, J.-C.; Chung, K.-W. Determination and application of combined genotype of simple sequence repeats (SSR) DNA marker for cultivars of *Cymbidium goeringii*. *Hortic. Sci. Technol.* **2012**, *30*, 278–285. [[CrossRef](#)]
10. Obara-Okeyo, P.; Kako, S. Genetic diversity and identification of *Cymbidium* cultivars as measured by random amplified polymorphic DNA (RAPD) markers. *Euphytica* **1998**, *99*, 95–101. [[CrossRef](#)]
11. LeCun, Y.; Bengio, Y.; Hinton, G. Deep learning. *Nature* **2015**, *521*, 436–444. [[CrossRef](#)]
12. Tian, C.; Xu, Y.; Fei, L.; Yan, K. Deep learning for image denoising: A survey. In Proceedings of the International Conference on Genetic and Evolutionary Computing, Springer, Singapore, 14–17 December 2018; pp. 563–572.
13. Albawi, S.; Mohammed, T.A.; Al-Zawi, S. Understanding of a convolutional neural network. In Proceedings of the 2017 International Conference on Engineering and Technology (ICET), Antalya, Turkey, 21–23 August 2017; pp. 1–6.
14. Cengil, E.; Çinar, A.; Güler, Z. A GPU-based convolutional neural network approach for image classification. In Proceedings of the 2017 International Artificial Intelligence and Data Processing Symposium (IDAP), Malatya, Turkey, 16–17 September 2017; pp. 1–6.
15. Dyrmann, M.; Karstoft, H.; Midtiby, H.S. Plant species classification using deep convolutional neural network. *Biosys. Eng.* **2016**, *151*, 72–80. [[CrossRef](#)]
16. Yalcin, H.; Razavi, S. Plant classification using convolutional neural networks. In Proceedings of the 2016 Fifth International Conference on Agro-Geoinformatics (Agro-Geoinformatics), Tianjin, China, 18–20 July 2016; pp. 1–5.
17. Ma, J.; Du, K.; Zheng, F.; Zhang, L.; Gong, Z.; Sun, Z. A recognition method for cucumber diseases using leaf symptom images based on deep convolutional neural network. *Comput. Electron. Agric.* **2018**, *154*, 18–24. [[CrossRef](#)]
18. Patel, I.; Patel, S. An Optimized Deep Learning Model for Flower Classification Using NAS-FPN and Faster R-CNN. *Int. J. Sci. Technol. Res.* **2020**, *9*, 5308–5318.
19. Liu, Y.H. Feature extraction and image recognition with convolutional neural networks. *J. Phys. Conf. Ser.* **2018**, *1087*, 062032. [[CrossRef](#)]
20. Workman, S.; Jacobs, N. On the location dependence of convolutional neural network features. In Proceedings of the IEEE Conference on Computer Vision and Pattern Recognition Workshops, Boston, MA, USA, 7–12 June 2015; pp. 70–78.
21. Li, W.; Wu, G.; Zhang, F.; Du, Q. Hyperspectral image classification using deep pixel-pair features. *IEEE Trans. Geosci. Remote Sens.* **2016**, *55*, 844–853. [[CrossRef](#)]
22. Hiary, H.; Saadeh, H.; Saadeh, M.; Yaqub, M. Flower classification using deep convolutional neural networks. *IET Comput. Vis.* **2018**, *12*, 855–862. [[CrossRef](#)]
23. Dias, P.A.; Tabb, A.; Medeiros, H. Apple flower detection using deep convolutional networks. *Comput. Ind.* **2018**, *99*, 17–28. [[CrossRef](#)]
24. Alaslani, M.G. Convolutional neural network based feature extraction for iris recognition. *Int. J. Comput. Sci. Inf. Technol. (IJCSIT)* **2018**, *10*, 65–78. [[CrossRef](#)]
25. Huang, K.; Liu, X.; Fu, S.; Guo, D.; Xu, M. A lightweight privacy-preserving CNN feature extraction framework for mobile sensing. *IEEE Trans. Dependable Secur. Comput.* **2019**, *18*, 1441–1455. [[CrossRef](#)]
26. Xie, G.-S.; Zhang, X.-Y.; Yang, W.; Xu, M.; Yan, S.; Liu, C.-L. LG-CNN: From local parts to global discrimination for fine-grained recognition. *Pattern Recognit.* **2017**, *71*, 118–131. [[CrossRef](#)]
27. Hao, X.; Jia, J.; Khattak, A.M.; Zhang, L.; Guo, X.; Gao, W.; Wang, M. Growing period classification of *Gynura bicolor* DC using GL-CNN. *Comput. Electron. Agric.* **2020**, *174*, 105497. [[CrossRef](#)]
28. Simonyan, K.; Zisserman, A. Very deep convolutional networks for large-scale image recognition. *arXiv* **2014**, arXiv:1409.1556.
29. Chao, X.; Sun, G.; Zhao, H.; Li, M.; He, D. Identification of apple tree leaf diseases based on deep learning models. *Symmetry* **2020**, *12*, 1065. [[CrossRef](#)]
30. Neupane, B.; Horanont, T.; Aryal, J. Deep Learning-Based Semantic Segmentation of Urban Features in Satellite Images: A Review and Meta-Analysis. *Remote Sens.* **2021**, *13*, 808. [[CrossRef](#)]

31. Zhou, Q.; Situ, Z.; Teng, S.; Chen, G. Convolutional Neural Networks—Based Model for Automated Sewer Defects Detection and Classification. *J. Water Resour. Plan. Manag.* **2021**, *147*, 04021036. [[CrossRef](#)]
32. Huang, K.; Li, C.; Zhang, J.; Wang, B. Cascade and Fusion: A Deep Learning Approach for Camouflaged Object Sensing. *Sensors* **2021**, *21*, 5455. [[CrossRef](#)]
33. Lin, G.; Shen, W. Research on convolutional neural network based on improved Relu piecewise activation function. *Procedia Comput. Sci.* **2018**, *131*, 977–984. [[CrossRef](#)]
34. Agarap, A.F. Deep learning using rectified linear units (relu). *arXiv* **2018**, arXiv:1803.08375.
35. Srivastava, N.; Hinton, G.; Krizhevsky, A.; Sutskever, I.; Salakhutdinov, R. Dropout: A simple way to prevent neural networks from overfitting. *J. Mach. Learn. Res.* **2014**, *15*, 1929–1958.
36. Hu, K.; Zhang, Z.; Niu, X.; Zhang, Y.; Cao, C.; Xiao, F.; Gao, X. Retinal vessel segmentation of color fundus images using multiscale convolutional neural network with an improved cross-entropy loss function. *Neurocomputing* **2018**, *309*, 179–191. [[CrossRef](#)]
37. Dozat, T. Incorporating nesterov momentum into adam. In Proceedings of the 4th International Conference on Learning Representations, Workshop Track, Caribe Hilton, San Juan, Puerto Rico, 2–4 May 2016.
38. Yu, W.; Yang, K.; Bai, Y.; Xiao, T.; Yao, H.; Rui, Y. Visualizing and comparing AlexNet and VGG using deconvolutional layers. In Proceedings of the 33rd International Conference on International Conference on Machine Learning, New York, NY, USA, 19–24 June 2016.
39. Ballester, P.; Araujo, R.M. On the performance of GoogLeNet and AlexNet applied to sketches. In Proceedings of the Thirtieth AAAI Conference on Artificial Intelligence, Phoenix, AZ, USA, 12–17 February 2016.
40. Gao, M.; Chen, J.; Mu, H.; Qi, D. A Transfer Residual Neural Network Based on ResNet-34 for Detection of Wood Knot Defects. *Forests* **2021**, *12*, 212. [[CrossRef](#)]
41. Yacouby, R.; Axman, D. Probabilistic Extension of Precision, Recall, and F1 Score for More Thorough Evaluation of Classification Models. In *Proceedings of the First Workshop on Evaluation and Comparison of NLP Systems*; Association for Computational Linguistics: Stroudsburg, PA, USA, 2020; Volume 202, pp. 79–91.
42. Azman, A.A.; Ismail, F.S. Convolutional Neural Network for Optimal Pineapple Harvesting. *ELEKTRIKA-J. Electr. Eng.* **2017**, *16*, 1–4.
43. Saleem, G.; Akhtar, M.; Ahmed, N.; Qureshi, W.S. Automated analysis of visual leaf shape features for plant classification. *Comput. Electron. Agric.* **2019**, *157*, 270–280. [[CrossRef](#)]
44. Liu, J.; Pi, J.; Xia, L. A novel and high precision tomato maturity recognition algorithm based on multi-level deep residual network. *Multimed. Tools Appl.* **2020**, *79*, 9403–9417. [[CrossRef](#)]
45. Esgario, J.G.M.; Krohling, R.A.; Ventura, J.A. Deep learning for classification and severity estimation of coffee leaf biotic stress. *Comput. Electron. Agric.* **2020**, *169*, 105162. [[CrossRef](#)]
46. Gao, Y.; Beijbom, O.; Zhang, N.; Darrell, T. Compact bilinear pooling. In Proceedings of the 2016 IEEE Conference on Computer Vision and Pattern Recognition (CVPR), Las Vegas, NV, USA, 27–30 June 2016; pp. 317–326.
47. Yuan, Z.-W.; Zhang, J. Feature extraction and image retrieval based on AlexNet. In Proceedings of the Eighth International Conference on Digital Image Processing (ICDIP 2016), Chengdu, China, 20–22 May 2016; p. 100330E.
48. Thenmozhi, K.; Reddy, U.S. Crop pest classification based on deep convolutional neural network and transfer learning. *Comput. Electron. Agric.* **2019**, *164*, 104906. [[CrossRef](#)]
49. Sethy, P.K.; Barpanda, N.K.; Rath, A.K.; Behera, S.K. Nitrogen deficiency prediction of rice crop based on convolutional neural network. *J. Ambient. Intell. Humaniz. Comput.* **2020**, *11*, 5703–5711. [[CrossRef](#)]
50. Yaqoob, M.K.; Ali, S.F.; Bilal, M.; Hanif, M.S.; Al-Saggaf, U.M. ResNet Based Deep Features and Random Forest Classifier for Diabetic Retinopathy Detection. *Sensors* **2021**, *21*, 3883. [[CrossRef](#)]